Volume 10, Issue 2, 2020, 5021 - 5027 ISSN 2069-5837
Biointerface Research in Applied Chemistry
www.BiointerfaceResearch.com
https://doi.org/10.33263/BRIAC101.021027
Original Review Article Open Access Journal
Received: 03.09.2019 / Revised: 11.01.2020 / Accepted: 14.01.2020 / Published on-line: 27.01.2020

A review on g-C_3N_4 based photo-catalyst for clean environment

Manas Ranjan Pradhan [1], Snehashis Panda [1], Binita Nanda [1,*]
[1]Department of Chemistry, Institute of Technical Education and Research, Siksha 'O' Anusandhan (Deemed to be University), Bhubaneswar, Odisha, India
*corresponding author e-mail address: ***binitananda@soa.ac.in*** | Scopus ID 53980125400

ABSTRACT
In recent years, our mother earth is facing drastic environmental and energy crisis. To resolve this crisis, the search for suitable strategy becomes a challenge to the sciencetific community. In this aspect, graphitic carbon nitride (g-C_3N_4) attracts the attention because of its super hardness, low density, chemical, thermal stability and biocompatibility. Among various analogues, g-C_3N_4 is considered as one of the most stable allotrope in the research hotspot drawn attention as metal-free and visible light responsive photocatalyst. Moreover, g-C_3N_4 acts as an n-type semiconductor and unique electrical, optical, structural and physiochemical properties. This makes g-C_3N_4 and g-C_3N_4 based materials, a new class of multifunctional nano platform. The polymeric structure of g-C_3N_4 enables the tuning of surface of g-C_3N_4 at a molecular level. However it has the lowest band structure among all the seven phases of CN. These properties enable the g-C_3N_4, an emerging and ideal candidate for clean energy production and environmental remediation. Last but not least, this review article emphasizes on the summary and some invigorative perspective on the challenges and future directions towards the development of sustainability without environmental detriment.

Keywords: *g-C_3N_4; photocatalysis; hydrogen energy generation.*

1. INTRODUCTION

In recent years, the global energy problem and environmental crisis are hindered the sustainability. This encouraged the scientists and researchers to develop some noble pathway for clean energy production as well as pollutants degradation strategies with the help of efficient photocatalytic materials [1]. Over the past decades semiconducting based visible light driven photocatalytic materials are the most suitable alternative that has attracted the attention of the researchers. Conversion of water into hydrogen is the best technique and regarded as a promising route with a higher efficiency [2, 3]. Many photocatalytic systems have been explored for efficient absorption, utilization, and conversion of solar photons in a sustainable and greener mode [4, 5]. A handful of semiconducting metals, metal oxides, and metal composites are extensively used as photocatalyst to harness solar energy (green technology) for cleaner environment. Among all, the story of semiconductor photocatalysis starts with $TiO_2$by Fujishima and Honda, and termed as 'golden' photocatalyst for a long period.

The large band-gap of TiO_2 (anatase) is 3.2 eV restrict the broad spectrum of sun light. To handle these problem, scientist and researchers have taken the challenges and search a new semiconducting visible light responsive material which tackle the environmental remediation and solve the energy crisis. Recently, a simple efficient, highly stable and sustainable polymeric material, graphitic carbon nitride (g-C_3N_4),a n-type semiconductor, taken as a metal-free visible light responsive photocatalyst for H_2 evolution and pollutant degradation. Berzelius was the first man to synthesize it and after that Liebig was named "MELON" [6]. But later on more simple and feasible method (thermal condensation) was implemented for synthesizing g-C_3N_4using nitrogen rich precursors like cyanamide, dicyandiamide, urea, thiourea and melamine as precursors [7]. It is a stable allotrope of carbon nitride as there is a strong covalent bond between carbon and nitrogen [8]. Another way it is a poly-conjugated semiconductor which contains earth's most abundant elements C and N atoms with a molar ratio C/N is 0.75, suggesting g-C_3N_4 is low cost material with two-dimensional stacking of π conjugated planes analogous to graphite. It is iso-structural with graphite where van der Waals' force holds the stacking layers (covalent C–N bonds) with each layer composed of tri-s-triazine units. It is bio-compatible, thermally and chemically stable in both acidic and alkaline environments. It has photo-electrochemical property in-oxidizability and waterproofing nature for which it is most wanted in photo-catalytic application and energy conservation [9-10]. Wang et al. synthesized bulk g-$C_3N_4$for the first time in 2009, using cyanamide were applied to photocatalytic H_2 generation from water [11]. After that, a number of review articles have been focused on the synthetic strategies of g-C_3N_4. Basing on the heat and chemical resistance, g-C_3N_4 exhibits unique stability. As prepared g-$C_3N_4$is non-volatile till the temperature reaches up to 600^0C, but completely decomposed at temperature 700^0C, confirm from thermogravimetry analysis (TGA) [12-14]. In single layer of g-C_3N_4, mainly consist of triazine and tri-s-triazine, is considered as tectonic unit [15]. Different synthesis methods such as hydrothermal, physical vapour deposition, chemical vapour deposition, solid state methods, and thermal condensation are commonly adopted. Among all, thermal condensation is the most commonly adopted technique, where basically nitrogen rich species are used as precursors. The most commonly used precursors are melamine, cyanamide, dicynamide, urea and thiourea etc [16]. When melamine undergoes thermal reaction, self-condensation occurs along with deammonication process and produces intermediate products such as melam, melem, and melon respectively. Which again thermal condensation at 400-5000C, g-C_3N_4 is formed, which is shown in scheme-1.

Despite the presence of many transition metal oxides like ZnO, TiO_2 which are active within UV region, corresponding to

an optical wavelength 460 nm, makes g-C_3N_4active under visible light. Clearly, it is seen that the band gap of g-C_3N_4 is 2.7eV.

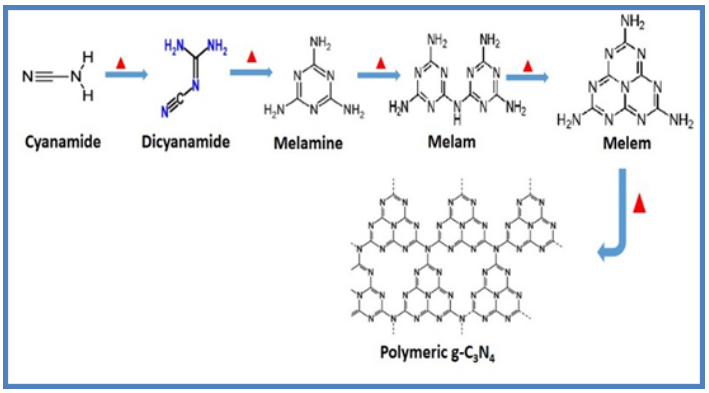

Scheme-1. Systematic approach synthesis of polymeric g-C_3N_4.

Due to thermodynamic losses and over potentials in the photocatalytic process the band gap lies between 2.1-3 eV, which enhances the hydrogen energy generation with enough endothermic driving force and light absorption in the visible region. Though g-C_3N_4has many applications towards clean energy and environment, but unfortunately its efficiency is low due to grain boundary effect, marginal absorption of visible light (< 460 nm), very low surface area (10 m^2g^{-1}), low quantum efficiency, high recombination rate of electron-hole pair less active sites for interfacial photon reactions, slow surface reaction kinetics, and low charge mobility interrupt electron delocalization [17]. Its photo-catalytic activity thus be enhanced by modifying its electronic structure by doping [18], templating [19], co-catalyzing [20], copolymerization [21], heterogeneous catalysis [22], and surface modification [23]. Amongstnumerous prospects, photocatalysis by establishing hetero-junction between twofold semiconductors, identified as Z-scheme photo-catalysis [24–25]. It has been fascinatedbecause of consumption ofa greatpercentage of the solar spectrum and reduces the rate of recombination by driving the redox process at different sites of the catalyst. Even photo-catalysis by doping is testified by Zhang et al. that phosphorus atoms is introduced into the framework of g-C_3N_4 by substituting C atoms [26-27]. As tri-s-triazine motif in g-C_3N_4 is considered to be electron acceptor, then P atom becomes electron rich and tri-s-tri-azine will be electron-deficient which is favourable for the effective separation of photo-generated e^- and h^+ pairs and improve the photo-catalytic efficiency [28-29].

In this book chapter, we are mainly focus on the green technology for a clean environment by pollution abetment and energy conservation. Basing on green technology, photocatalysis is the safer, cleaner and greener method to reduce the environmental hazards and give an alternative path for hydrogen evolution to mitigate the energy crisis. Taking this into consideration, finding a suitable catalyst is a challenging task. In this way, g-C_3N_4 is a very good photocatalyst for hydrogen generation and pollutant degradation. This book chapter, also provide a comprehensive recent data generated by different authors regarding photocatalysis and energy evolution.

2. RESULTS

Photocatalysis: A Promising route for energy and environment

Photocatalysis

The goal of 21st century chemistry is to adopt energy efficient routes to avoid environmentally hazardous processes with replacement of harmful chemicals during production and uses. Photocatalysis, a conventional green technology, the advanced oxidation process (AOP) has the pivotal role in today's clean environmental [30]. As definition denotes, photocatalysis is a 'green' technique which accelerates the photoelectron in the presence of promoter. In the photocatalytic reaction, light is absorbed by an adsorbed substrate. Therefore, in photo generated catalysis, semiconducting nano materials preferred as photocatalyst due to narrow band gap between the valance band and conduction band [31-32].

Mechanism

Semiconducting materials having filled valence band (occupied by electrons) and an empty conduction band (unoccupied electronic states) are mostly sensitizes redox processes in presence of light. The two bands are separated by an energy gap particular to each semiconductor referred to as the band gap (E_g). In the photocatalytic process, when a semiconducting material is subjected to radiation exceeding its band gap, establishing a redox environment. This helps in generation of e^- and h^+ pairs in the valance band and conduction band [33-34]. These e^- and h^+ pairs enable redox reaction and form different oxidative radicals on surface of semiconductor and enhance the photocatalysis process through three mechanistic ways such as: proper excitation, bulk diffusion and surface charge transfer [35].

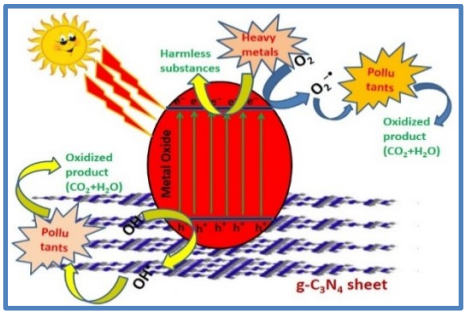

Scheme 2. Mechanism of photocatalysis reaction process.

In a typical photocatalytic process, when the semiconductor photocatalyst is illuminated with light of sufficient energy (either UV/visible light source), the e^-s of VB jumped to the CB, thus leaving an h^+ in VB is shown in scheme-1. The holes (h^+) produced in VB, are trapped by the surface adsorbed water molecule and generates $OH^•$ radical. At the same time photo generated electrons (e^-) in CB react with the dissolved oxygen forming superoxide radical ($O_2^{-•}$), which again reacts with photon (H^+) to produce hydroperoxyl radical ($HO_2^•$) followed by the formation of H_2O_2. The charge transfer and production of highly oxidative radicals during the redox process enhances the photocatalytic ability of a semiconductor. The mechanism of photocatalysis is explained below and the schematic representation is shown in scheme-2

$$\text{Photocatalyst} + h\upsilon \rightarrow e^- (CB) + h^+ (VB) \quad (1)$$

$$OH^- + h^+ (VB) \rightarrow OH^• \quad (2)$$

$$O_2 + e^- (CB) \rightarrow O_2^{-•} \quad (3)$$

$$O_2^{-•} + H^+ \rightarrow HO_2^• \quad (4)$$

$$2\,HO_2^• \rightarrow H_2O_2 + O_2 \quad (5)$$

$$H_2O_2 + e^- (CB) \rightarrow OH^• + OH^- \quad (6)$$

In this regard, the electronic structure of g-C_3N_4 accountable the photocatalytic ability. The presence of two abundant element carbon and nitrogen in g-C_3N_4 and the lone pair electron of nitrogen plays an important role in electronic structure. The combination of π bonding electronic states and the lone pair of nitrogen stabilizes the electronic lone pair state [36]. The role of nitrogen content in optical properties of g-C_3N_4 was again confirmed by Abd El-Kader et al. [37]. To enhance the positive improvement in optical properties and photocatalytic performance, band gap is to be modified with negative ions in g-C_3N_4 by doping [38] as the position of VB and CB are responsible for oxidation and reduction levels. Generally, the HUMO –LUMO band gap of melem is 3.5 eV and it is reduced to 2.6 eV in case of melon and finally attain the band gap 2.1 eV with fully formation of condensed g-C_3N_4. The wave function investigated that the nitrogen Pz orbitals and carbon Pz orbitals drove VB and CB, where the photogenerated e^-s and h^+s are separated. This creates the oxidation and reduction cites in VB and CB respectively, which is responsible for splitting of water (H_2 generation) and pollutant degradation independently in the nitrogen and carbon atom.

Wei et al. synthesized visible light responsive photocatalyst mesoporous TiO_2/g-C_3N_4 for phenol degradation. Amorphous TiO_2 microsphere was coated with thin layer of g-C_3N_4 was clearly visible from SEM and TEM study. From HRTEM, it is clear that heterojunction formed due to the connection of the crystal lattice of TiO_2 and g-C_3N_4 at the interface of TiO_2/g-C_3N_4. The irregular mesoporosity of TiO_2 and the composites (TiO_2/g-C_3N_4) were confirmed from N_2 adsorption and desorption study, which exhibited the type (IV) isotherm. UV-vis DRS shows that the light absorption of TiO_2 was restricted to wavelength range at 390 nm. But, after the decoration of g-C_3N_4 on the surface of TiO_2 extended the absorption of light towards visible region. The PL spectra of TiO_2 was found to be in the range 350-420 nm due to band-band emission and surface oxygen vacancy effect. In the case of TiO_2/g-C_3N_4 composite the peak intensity was negligible which confirms the reduction of electron-hole recombination rate by the efficient separation of electron-hole pairs. During the photocatalytic degradation of phenol, there is a charge transfer through TiO_2/g-C_3N_4 heterojunction. The heterojunction was formed inside the anatase of TiO_2 structure, the growth of g-C_3N_4 was restricted and only a thin layer of g-C_3N_4 was embedded on the surface of TiO_2. During the addition of precursor (cyanamide) and the intermediate product (melem and s-triazine) possibly react with TiO_2 and form $TiO_{2-x}N_x$ after calcination (well confirmed through XPS). In the heterojunction both g-C_3N_4 and TiO_2-xNx are irradiated under visible light, generates electron-hole pair. During this process, the transfer of electrons occurs from CB of g-C_3N_4 to CB of TiO_2-xNx, whereas the holes present in the VB of TiO_2-xNx move towards VB of g-C_3N_4. The electrons accumulated in the CB of g-C_3N_4 and TiO_2-xNx react with atmospheric oxygen to produce superoxide radical (O_2^{-}), which responsible for the degradation of phenol [39].

Sun et al. fabricated g-C_3N_4/ZnO photocatalyst with different ZnO content for decomposition of para nitrophenol and methyl orange. The thermal stability and weight of g-C_3N_4/ZnO deceases, when the temperature rises from 520^0-690^0C. This shows that at temperature 500^0C, the composite is stable and above that combustion occurs and the weight of the g-C_3N_4 decreases and at the same time ZnO increases. This again confirms from PXRD which reveals that the intensity of peak of ZnO in the composite increases with increasing calcination time. The bonding between ZnO and g-C_3N_4 is probably due to condensation reaction between amino group of tri-s-triazine of g- C_3N_4 and surface OH group of ZnO. From HRTEM image it was revealed that there is an interface between g- C_3N_4 and hexagonal wurtzite phase of ZnO. UV-vis spectroscopy discloses that the absorption shift to the lower region to 470 nm corresponds to band gap of the composite is 2.8 eV. This arises due to the strong chemical bond between ZnO and g- C_3N_4 and enhances the photocatalytic activity towards methyl orange and paranitro phenol. Increasing Zn content in the composite, remarkably enhances the photocatalytic activity. The photocatalytic activity of the composite is found to be increasing with increase in ZnO content as degradation of MO is about 97% for 16 wt% of ZnO in g-C_3N_4 in 80 min. This shows that there is a strong synergism between ZnO and g-C_3N_4 in g-C_3N_4/ZnO photocatalyst. The increased photocatalytic property of g-C_3N_4/ZnO is due to lower –ve conduction band potential of g-C_3N_4 (-1.12eV) than that of ZnO (0.5 eV). Photo induced e^-s on conduction band of g-C_3N_4 goes to that of ZnO through the interface and produces O_2^{-} from atmospheric oxygen. MO degradation charged the g-C3N4 surface and again restore to the ground state. The two semiconductor also rebuild the electric field and creates the electron-hole separation, which accumulates a large number of electron on the surface of ZnO and enhances the photocatalytic activity towards MO degradation [40].

He et al. fabricated Z-scheme type MoO_3/g-C_3N_4 photocatalysts and evaluated for its photo degradation activities towards methyl orange (MO). From thermo gravimetric analysis shows that there is a weight loss in the composites as g-C_3N_4 volatilized within temperaure range of 600-750^0C. Again vaporization of MoO_3 in the composites (MoO_3/g-C_3N_4) further loss the weight occurs within 750 to 800^0C. The surface areas of MoO_3/g-C_3N_4 composites are more as compared pure MoO_3 and pure g-C_3N_4. The surface area of the composite (MoO_3/g-C_3N_4) increases due to the modification of MoO_3 grains on the surface of g-C_3N_4 is and again decreases due to agglomeration of a higher amount of MoO_3 onto the surface of g-C_3N_4. UV-vis DRS spectra delineates the optical properties of MoO_3/g-C_3N_4 fall in between those of MoO_3 and g-C_3N_4. This is because of both MoO_3 and g-C_3N_4 possess nearly equal band gap. For this reason both the semiconductors exhibit nearly the same photo absorbance. MoO_3 shows less photocatalytic activity towards MO, after modification with g-C_3N_4 the activity increases. As the % of MoO_3 increases the photocatalytic activity of MO increases (1.5 wt % is the highest) and again decreases because at high wt % of MoO_3 (2 wt %) on g-C_3N_4 may block the visible light absorbance and decreases the degradation percentage. Furthermore MoO_3/g-C_3N_4 obeys the Z-scheme mechanism as $O_2^{-\bullet}$ and h^+ the two active species during photocatalytic degradation of MO [41].

(II) Photocatalytic water spiltting:

In recent year, production of clean energy is a big challenge. The conversion of solar energy to chemical energy is the most suitable greener method to mitigate the future energy crisis in cleaner way. This is because when hydrogen gas is burned as fuel, water vapour is released, which restricts global warming

and emission of other air pollutants. In this regard, photocatalytic water splitting, is the alternative way to conserve energy sources. Because in this process relies on sunlight and semiconductor and considered as solar-to-hydrogen conversion (STH). This can be calculated as:

STH = Output energy as H_2/ energy of incident solar light (7)

Apparent quntum efficiency is the appropriate method to evaluate the photocalytic performance

AQY=nR/I (8)

Where, n is the number of electrons involved, R is the rate of production of H_2 and I is the rate of incident radiation (photons).

For photocatalytic hydrogen generation photochemical or photoelectrical cells are generally used but thermodynamically the process is difficult due to very high change in free energy of the process which is about +237.2kj/mole. For the generation of hydrogen basically three steps are used. First of all electron-hole pair is to be produced by absorption of light with energy equal or greater than band gap energy of photocatalyst. Secondly, the electron-hole pairs called charge carriers to migrate to the surface of photocatalyst or combine in the core. Last of all the photogenerated electron in CB reduces water to liberate hydrogen whereas the holes oxidise water molecules to liberate oxygen at VB [42]. The mechanism of the reaction is given below and explained through schematic diagram 3.

$2H_2O + 4\ h\upsilon \rightarrow 2H_2 + O_2$ (9)

$4H^+ + 4e^- \rightarrow 2H_2$ (reaction at CB) (10)

$H_2O \rightarrow 2h^+ \rightarrow O_2$ (reaction at VB) (11)

Qin eta al. developed a heterostructure photocatalyst by coupling Cu_3P with g-C_3N_4 which are p and n type semiconductors respectively for effective charge separation there by improving photocatalytic hydrogen generation. This heterocatalyst shows 95 times more activity than bare g-C_3N_4 with AQE of 2.6% at 420 nm. As Cu_3P has low cost and is earth abundant with a band gap of 1.5 eV that can improve the charge separation and enhance photocatalytic performance of g-C_3N_4. Hydrogen generation by g-C_3N_4 is faint but adding Cu_3P increases the rate of hydrogen production which is about 95.7 times higher than bulk g-C_3N_4. It is to be noted that Cu_3P is not an active photocatalyst but mixture of Cu_3P and g-C_3N_4 increases slightly the generation of hydrogen but when a heterojunction is formed between Cu_3P and g-C_3N_4 the production of hydrogen increases many more times. It is evident from SPV spectra. The SPV signal identifies the light response of wavelength range and how efficiently the charged pairs are separated in the photocatalyst. The spectroscopic and electrochemical analysis says that the heterojunction possesses efficient charge separation capacity which facilitates photochemical activity. When Cu_3P is loaded over g-C_3N_4 an electron transfers from g-C_3N_4 to Cu_3P takes place until the Fermi level becomes equal. When the heterojunction photocatalyst is exposed to visible light, the photogenerated electrons in CB of Cu_3P diffuses into CB of g-C_3N_4 through p-n junction. Simultaneously the photogenerated holes in VB of g-C_3N_4 diffuses into VB of Cu_3P. Now the electron in g-C_3N_4 reduces H^+ ion liberating hydrogen and holes oxidizes water to liberate oxygen henceforth justifying water splitting capability [43].

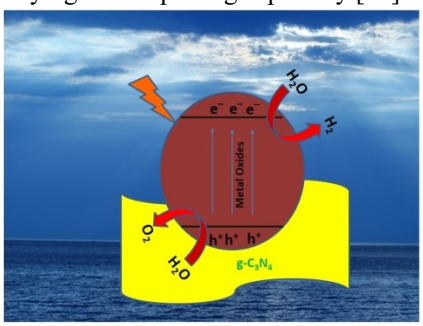

Scheme 3. Schematic representation of H_2 gas generation.

Wang and his team have synthesized g-C_3N_4 and Mn doped g-C_3N_4 nanoribbon for photocatalytic degradation of MB coupling with water splitting. The controlled synthesis of Mn doped g-C_3N_4 allows better results compared to bulk g-C_3N_4. HRTEM confirms the nanoribbon morphology of Mn doped g-C_3N_4 with high surface area 134 m^2/g as compared to bulk g-C_3N_4 (58.7 m^2/g). The successful doping of Mn onto the surface of g-C_3N_4 was observed by XPS and EDS mapping. From the band gap of both g-C_3N_4 and Mn doped g-C_3N_4 nanoribbon (2.67 and 2.56 eV respectively) confirms that both are visible light active. Mn dped g-C_3N_4 nanoribbon shows better H_2 and O_2 yield (380.39 and 74.78 µmol/gcat) respectively. Again coupling of photocatalytic performance and water splitting shows better results in the case of Mn doped g-C_3N_4 nanoribbon. This is because construction of nanoribbon and doping of Mn helps in separation of electron ad hole in the photocatalyst. Mainly doping of Mn facilitates the formation of $OH^{\bullet}$ from H_2O_2 intermediate product. The coupling reaction solves the problem of H_2O_2 production and offers the possibility of energy utilization mode of waste water [44]. Different materials used in photocatalysis process are summarized in the Table 1.

Table-1. Tabulations of different synthetic methods of g-C_3N_4 based composites and their applications.

S.L. No	Catalysts	Methods of Synthesis	Application	References
1	Na-doped g-C_3N_4	Solid state method	Photodegradation of 17α-ethynylestradiol	45
2	Cu (I) – g-C_3N_4	Wet impregnation-ultrasonication method	Photodegradation of atrazine	46
3	g-C_3N_4 – WO_3	Hydrothermal method	H_2 energy production	47
4	Se – doped g-C_3N_4	Ultrasonication method	H_2- production	48
5	g-C_3N_4/Silica gels	Solvothermal method	White light emitting devices	49
6	g-C_3N_4	Pyrolysis process	Photo electrochemical sensing of methylene blue	50
7	MnO_2/Ag/g-C_3N_4	Hydrothermal method	Photoreduction of CO_2	51
8	g-C_3N_4/Bi_2WO_6	Hydrothermal method	CO_2 photoreduction	52
9	g-C_3N_4-Ti_3C_2Tx	Calcination process	H_2 evolution	53
10	CuO/g-C_3N_4	Sonication process	4-nitrophenol degradation and O_2 evolution	54
11	g-C_3N_4-TiO_2	Stirring followed by calcination	Methylene blue degradation	55
12	NiO/g-C_3N_4	Hydrothermal	Photocatalytic water splitting	56
13	WO_3-g-C_3N_4	Hydrothermal	Sulfamethoxazole degradation	57

S.L. No	Catalysts	Methods of Synthesis	Application	References
14	MoS_2-QDs/g-C_3N_4	Wetness impregnation method	H_2 evolution	58
15	TiO_2-g-C_3N_4	Hydrothermal method	Organic pollutant degradation	59
16	WO_3-g-C_3N_4	Calcination process	Degradation of methylene blue and 4-chlorophenol	60
17	N-TiO_2-g-C_3N_4	Impregnation method	H_2 evolution	61
18	g-C_3N_4-BiOBr	Ultrasonic method	Pollutant degradation	62
19	3C-SiC/g-C_3N_4	Pyrolysis method	Degradation of methyl orange	63
20	PANI-g-C_3N_4	Oxidative polymerization process	Methylene blue degradation	64

4. CONCLUSIONS

In summary, this review article mainly highlights green technology for clean environment. In this regard, g-C_3N_4 based composites are proven to be a good photocatalyst for environmental remediation and energy recovery. To this end, the enhancement of photocatalytic performance of g-C_3N_4 is mainly due to three factors such as: 1) visible light responsive, ii) low rate of recombination of photoinduced charge carriers, and iii) high surface area. These above properties enable to anchor different foreign materials on the surface of g-C_3N_4 nanosheet and further activate the performance. This review summarizes a bunch of recent work was done by the scientist. So, g-C_3N_4 based composites are considered as the best material for future generation sustainability.

5. REFERENCES

1. Chaturvedi, S.; Dave, P.N. Environmental application of photocatalysis. *Materials Science Forum* **2012**, *734*, 273-294, https://doi.org/10.4028/www.scientific.net/MSF.734.273
2. Sahoo, D.P.; Patnaik, S.; Rath, D.; Nanda, B.; Parida, K.M. Cu@CuO promoted g-C_3N_4/MCM-41: an efficient photocatalyst with tunable valence transition for visible light induced hydrogen generation. *RSC Advances* **2016**, *6,* 112602-112613, https://doi.org/10.1039/C6RA24358D.
3. Sahoo, D.P.; Rath, D. Nanda, B. Parida, K.M. Transition metal/metal oxide modified MCM-41 for pollutant degradation and hydrogen energy production. *RSA Advances* **2015**, *5*, 83707-83724, https://doi.org/10.1039/C5RA14555D.
4. Wang, Y.; Zhang, Y.; Zhao, S.; Huang, Z.; Chen, W.; Zhou, Y. Bio template synthesis of Mo-doped polymer carbon nitride for photocatalytic hydrogen evolution. *Applied catalysis B: Environmental* **2019**, *248,* 44-53, https://doi.org/10.1016/j.apcatb.2019.02.007
5. Lai, C.; Zhang, M.; Li, B.; Huang, D.; Zeng, G.; Liu, X.; Chen, L. Fabrication of CuS/$BiVO_4$ binary heterojunctions photocatalysts with enhanced photocatalytic activity for ciprofloxacin degradation and mechanism insight. *Chemical Engineering Journal* **2019**, *358,* 891-902, https://doi.org/10.1016/j.cej.2018.10.072.
6. Liu, A.Y.; Cohen, M.L. Prediction of new low compressibility solids. *Science* **1989**, *245*, 841-842, https://doi.org/10.1126/science.245.4920.841.
7. Wang, X.; Zhang, G.; Lan, Z.A. A facile synthesis of Br modified g-C_3N_4 semiconductors for photoredox water splitting. *Applied Catalysis B: Environmental* **2016**, *192,* 116-125, https://doi.org/10.1016/j.apcatb.2016.03.062.
8. Sierra, U.; Alvarez, P.; Blanco, C. New alternatives to graphite for producing graphene materials. *Carbon* **2015**, *93*, 812-818, https://doi.org/10.1016/j.carbon.2015.05.105.
9. Li, X.; Dai, Y.; Ma, Y. Graphene/g-C_3N_4 bilayer considerable band gap opening and effective band structure engineering. *Phys Chem Chem Phys* **2014**, *16*, 4230-4235, http://dx.doi.org/10.1039/c3cp54592j.
10. Tian, Y.; Chang, B.; Lu, J. Hydrothermal synthesis of graphitic carbon nitride-Bi_2WO_6 heterojunctions with enhanced visible light photocatalytic activities. *ACS Applied Material & Interfaces* **2013**, *5*, 7079-7085, https://doi.org/10.1021/am4013819.
11. Xiong, M.; Chen, L. Yuan, Q. Controlled synthesis of graphitic carbon nitride/beta bismuth oxide composite and its high visible light photocatalytic activity. *Carbon* **2015**, *86,* 217-224, https://doi.org/10.1016/j.carbon.2015.01.023.
12. He, F.; Chen, G.; Wang, Z.; Su, D.; Liu, S.; Zhang, L. Sulfur mediated self templating synthesis of tapered C-PAN/g-C_3N_4 composite nanotubes toward efficient photocatalytic hydrogen evolution. *ACS Energy Lett* **2016**, *5*, 969-975, https://doi.org/10.1021/acsenergylett.6b00398.
13. Lu, Y.; Ji, C.; Li, Y.; Qu, R.; Sun, C.; Zhang, Y. Facile one pot synthesis of C and g-C_3N_4 composites with enhanced photocatalytic activity using hydroxymethylated melamine as carbon source and soft template. *Materials Letters* **2018**, *211*, 78-81, https://doi.org/10.1016/j.matlet.2017.09.080.
14. Li, L.; Sun, S.Q.; Wang, Y.X.; Wang, C.Y. Facile synthesis of ZnO/g-C_3N_4 composites with honeycomb like structure by hydrogen bubble templates and their enhanced visible light photocatalytic performance. *Journal of photochemistry and photobiology A: Chemistry* **2018**, *355*, 16-24, http://dx.doi.org/10.1016/j.jphotochem.2017.12.016.
15. Li, K.; Gao, S.; Wang, Q.; Wang, Z.; Huang, B.; Jun, L. In-situ-reduced synthesis of Ti^{+3} self doped TiO_2/g-C_3N_4 heterojunctions with high photocatalytic performance under LED light irradiation. *ACS Appl. Mater. Interfaces* **2015**, *7,* 9023-9030, https://doi.org/10.1021/am508505n.
16. Xue, J.; Ma, S.; Zhou, Y.; Zhang, Z.; He, M. Facile photochemical synthesis of Au/Pt/g-C_3N_4 with plasmon enhanced photocatalytic activity for antibiotic degradation. *ACS Appl. Mater. Interfaces* **2015**, *7*, 9630-9637, https://doi.org/10.1021/acsami.5b01212.
17. Xu, M.; Han, L.; Dong, S. Facile fabrication of highly efficient g-C_3N_4/Ag_2O heterostructured photocatalysts with enhanced visible-light photocatalytic activity. *ACS Appl. Interfaces* **2013**, *5*, 12533-12540, http://dx.doi.org/10.1021/am4038307.
18. Han, H.; Fu, Min.; Li, Y.; Guan, W.; Lu, P.; Hu, X. Insitu polymerization for PPy/g-C_3N_4 composites with enhanced visible light photocatalytic performance. *Chinese Journal of Catalysis* **2018**, *39*, 831-840, https://doi.org/10.1016/S1872-2067(17)62997-8.
19. Kumar, S.; Karthikeyan, S.; Lee, F.A. g-C_3N_4 based nanomaterials for visible light driven photocatalysis. *Catalysts* **2018**, *8,* 74, https://doi.org/10.3390/catal8020074.
20. Ren, S.; Chen, C.; Zhou, Y.; Dong, Q.; Ding, H. The α-Fe_2O_3/g-C_3N_4 composite as an efficient heterogeneous catalyst with combined fenton and photocatalytic effects. *Research on Chemical Intermediates* **2016**, *43,* 3307-3323, http://dx.doi.org/10.1007/s11164-016-2827-x.
21. Chen, Y.; Lin, B.; Wang, H.; Yang, Y.; Zhu, H.; Yu, W. Surface modification of g-C_3N_4 by hydrazine: simple way of

noble metal free hydrogen evolution catalysts. *Chemical Engineering Journal* **2016**, *286,* 339-346, https://doi.org/10.1016/j.cej.2015.10.080.
22. Yang, L.; Huang, J.; Shi, L.; Cao, L.; Yu, Q.; Jie, Y. A surface modification resultant thermally oxidized porous g-C_3N_4 with enhanced photocatalytic hydrogen production. *Applied Catalysis B: Environmental* **2017**, *204*, 335-345, https://doi.org/10.1016/j.apcatb.2016.11.047.
23. Liu, Y.; Zhang, H.; Ke, J.; Zhang, J.; Tian, W.; Xu, X.; Duan, X.; Sun, H. MoS_2/g-C_3N_4 heterojunctions in Z- Scheme for enhanced photocatalytic and electrochemical hydrogen evolution. *Applied catalysis B: Environmental* **2018**, *228*, 64-74, https://doi.org/10.1016/j.apcatb.2018.01.067.
24. Safaei, J.; Ullah, H.; Mohamed, N.A. Enhanced photoelectrochemical performance of Z-scheme g-C_3N_4/$BiVO_4$ photocatalyst. *Applied Catalysis B: Environmental* **2018**, *234*, 296-310, https://doi.org/10.1016/j.apcatb.2018.04.056.
25. Mishra, A.; Mehta, A.; Basu, S.; Shetti, N.P.; Reddy, K.R. Graphitic carbon nitride based metal free photocatalysts for water splitting. *Carbon* **2019**, *149,* 693-721, https://doi.org/10.1016/j.carbon.2019.04.104.
26. Zhu, B.; Zhang, L.; Cheng, B.; Yu, J. First principle calculation study of tri-s-triazine based g-C_3N_4. *Applied Catalysis B: Environmental* **2018**, *224,* 983-999, https://doi.org/10.1016/j.apcatb.2017.11.025.
27. Zou, H.; Yan, X.; Ren, J.; Wu, X.; Dai, Y. Photocatalytic activity enhancement of modified g-C_3N_4 by ionothermal co-polymerization. *Journal of Materiomics* **2015**, *1*, 340-347, https://doi.org/10.1016/j.jmat.2015.10.004.
28. Wei, W.; Jacob, T. Strong exitonic effects in the optical properties of graphitic carbon nitride from first principles. *Physical Review B* **2013**, *87,* 085202, http://dx.doi.org/10.1103/PhysRevB.87.085202.
29. Gong, Y.T.; Li, M.M. Wang, Y. Carbon nitride in energy conversion and storage: recent advances and future prospects. *ChemSusChem* **2015**, *8,* 931-946, https://doi.org/10.1002/cssc.201403287.
30. Chen, X.; Mao, S.S. Titanium dioxide nanomaterials: synthesis, properties, modification, and applications. *Chemical Reviews* **2007**, *107,* 2891-2959, https://doi.org/10.1021/cr0500535.
31. Niu, M.; Huang, F.; Cui, L.; Huang, P.; Yu, Y.; Wang, Y. Hydrothermal synthesis, structural characteristics, and enhanced photocatalysis of SnO_2/α-Fe_2O_3 semiconductor nanoheterostructures. *ACS Nano* **2010**, *4*, 681-688, https://doi.org/10.1021/nn901119a.
32. Anandan, S.; Ikuma, Y.; Niwa, K. An overview of semiconductor photocatalysis:modification of TiO_2 nanomaterials. *Solid state phenomena* **2010**, *162*, 239-260, https://doi.org/10.4028/www.scientific.net/SSP.162.239.
33. Nanda, B.; Pradhan, A.C.; Parida, K.M. A comparative study on adsorption and photocatalytic dye degradation under visible light irradiation by mesoporous MnO_2 modified MCM-41 nanocomposite. *Microporous and Mesoporous Materials* **2016**, *226,* 229-242, https://doi.org/10.1016/j.micromeso.2015.12.027.
34. Nanda, B.; Pradhan, A.C.; Parida, K.M. Fabrication of mesoporous CuO/ZrO2-MCM-41 nanocomposites for photocatalytic reduction of Cr (VI). *Chemical Engineering Journal* **2017**, *316,* 1122-1135, https://doi.org/10.1016/j.cej.2016.11.080.
35. Pradhan, A.C.; Nanda, B.; Parida, K.M.; Rao, G.R. Fabrication of the Mesoporous Fe@MnO_2NPs−MCM-41Nanocomposite: An Efficient Photocatalyst for Rapid Degradation of Phenolic Compounds. *J. Phys. Chem. C.* **2015,** *119,* 14145-14159, https://doi.org/10.1021/acs.jpcc.5b01907.
36. Wen, J.; Xie, J.; Chen, X.; Lia, X. A review on g-C_3N_4-based photocatalysts. *Applied Surface Science* **2017**, *391*, 72–123, https://doi.org/10.1016/j.apsusc.2016.07.030.
37. Abd El-kader, F.H.; Moharram, M.A.; Khafagia, M.G.; Mamdouh, F. A fantastic graphitic carbon nitride material: electronic structure, photocatalytic and photoelectronic properties. *Spectrochim. Acta A: Mol. Biomol. Spectrosc*. **2012**, *97*, 1115–1119, https://doi.org/10.1016/j.jphotochemrev.2014.04.002.
38. Dong, G.; Zhang, Y.; Pan, Q.; Qiu, J. A fantastic graphitic carbon nitride (g-C3N4) material: Electronic structure, photocatalytic and photoelectronic properties. *Journal of Photochemistry and Photobiology C: Photochemistry Reviews* **2014**, *20,* 33–50, https://doi.org/10.1016/j.jphotochemrev.2014.04.002.
39. Hao, W.; McMaster, W.A.; Jeannie, Z.Y.; Tan, L.C.; Dehong, C.; Caruso, R.A. Mesoporous TiO_2/g-C_3N_4 Microspheres with Enhanced Visible-Light Photocatalytic Activity. *J. Phys. Chem. C.* **2017**, *121*, 22114-22122, https://doi.org/10.1021/acs.jpcc.7b06493.
40. Sun, J.X.; Yuan, Y.P.; Qiu, L.G. Fabrication of composite photocatalyst g-C_3N_4-ZnO and enhancement of photocatalytic activity under visible light. *Dalton Transactions* **2012**, *41*, 6756, https://doi.org/10.1039/c2dt12474b.
41. He, Y.; Zhang, L.; Wang, X.; Wu, Y. Enhanced photodegradation activity of methyl orange over Z-scheme type MoO_3/g-C_3N_4 composite under visible light irradiation. *RSC Advances* **2014**, *4*, 13610-13619, https://doi.org/10.1039/C4RA00693C
42. Cao, S.; Yu, J. g-C_3N_4 Based Photocatalysts for Hydrogen Generation. *J. Phys. Chem. Lett.* **2014**, *5,* 2101−2107, https://doi.org/10.1021/jz500546b
43. Qin, Z.; Wang, M.; Li, R. Novel Cu3P/g-C3N4 p-n heterojunction photocatalystsfor solar hydrogen generation. *Sci China Mater* **2018**, *61*, 861–868, https://doi.org/10.1007/s40843-017-9171-9.
44. Wang, J.C.; Cui, C.X.; Kong, Q.Q.; Ren, C.Y.; Li, Z. Mn Doped g-C_3N_4 Nanoribbon for Efficient Visible-Light Photocatalytic Water Splitting Coupling with Methylene Blue Degradation. *ACS sustainable Chemistry & Engineering* **2018**, *6*, 8754-8761, https://doi.org/10.1021/acssuschemeng.8b01093.
45. Sudrajat, H. A one pot solid state route for realizing highly visible light active Na-doped g-C_3N_4 photocatalysts. *Journal of solid state chemistry* **2018**, *257*, 26-33, https://doi.org/10.1016/j.jssc.2017.09.024.
46. Sudrajat, H. Reducing agent free formation of Cu (I) nanoclusters on g-C_3N_4 for enhanced photocatalysis. *Journal of alloys and compounds* **2017**, *716,* 119-127, https://doi.org/10.1016/j.jallcom.2017.04.302.
47. Tahir, M.B.; Khan, M.I.; Majid, A.; Farooq, M. Enhanced photocatalytic hydrogen energy production of g-C_3N_4-WO_3 composites under visible light irradiation. *International Journal of Energy Research* **2018**, *42*, 4667-4673, https://doi.org/10.1002/er.4208.
48. Dante, R.C.; Vaquero, F. A simple approach to synthesize g-C_3N_4 with high visible light photoactivity for hydrogen production. *Internation Journal of Hydrogen Energy* **2015**, *40*, 7273-7281, https://doi.org/10.1016/j.ijhydene.2015.04.063.
49. Wang, A.; Lee, C.; Bian, H.; Li, Z. Synthesis of g-C_3N_4/Silica gels for white light emitting devices. Particle and *Particle Systems Characterization* **2016**, *34*, 1600258, https://doi.org/10.1002/ppsc.201600258.
50. Mo, Z.; She, X.; Huang, L. Synthesis of g-C_3N_4 at different temperatures for superior Visible/UV photocatalytic performance and photoelectrochemical sensing of MB solution. *RSC Advances* **2015**, *5*, 101552-101562, https://doi.org/10.1039/C5RA19586A.

51. Han, T.; Xie, C.; Wei, Y. Synthesized MnO_2/Ag/g-C_3N_4 composite for photoreduction carbon dioxide under visible light. *Journal of Materials Science: Materials in Electronics* **2018**, *29,* 20984-20990, https://doi.org/10.1007/s10854-018-0243-2.
52. Zhang, M.; Zhou, Y.; Shi, J. Highly selective CO_2 photoreduction to CO over g-C_3N_4/Bi_2WO_6 composites under visible light. *Journal of Materials Chemistry A* **2015**, *3*, 5189-5196, https://doi.org/10.1039/C4TA06295G.
53. Sun, Y.; Jin, D.; Sun, Y. g-C_3N_4/Ti_3C_2Tx composite with oxidized surface groups for efficient photocatalytic hydrogen evolution. *Journal of Materials Chemistry A* **2018**, *6*, 9124-9131, https://doi.org/10.1039/C8TA02706D.
54. Verma, A.; Jaihindh, D.P. Photocatalytic 4-nitrophenol degradation and oxygen evolution reaction in CuO/g-C_3N_4 composites prepared by deep eutectic solvent assisted chlorine doping. *Dalton Transactions* **2019**, *48,* 8594-8610, https://doi.org/10.1039/C9DT01046G.
55. Qiu, J.; Feng, Y. Zhang, X. Facile stir-dried preparation of g-C_3N_4/TiO_2 homogeneous composites with enhanced photocatalytic activity. *RSC Advances* **2017**, *7*, 10668-10674 https://doi.org/10.1039/C7RA00050B.
56. Liu, C.; Zhu, C.; Wang, H. High performance NiO/g-C_3N_4 composites for Visible light driven photocatalytic overall water splitting. *Inorganic Chemistry Frontiers* **2018**, *5*, 1646-1652, https://doi.org/10.1039/C8QI00292D.
57. Sun, F.; Goei, R.; Zhou, Y. Construction of WO_3-g-C_3N_4 composites as efficient photocatalysts for pharmaceutical degradation under Visible light. *Catalysis Science and Technology* **2017**, *7*, 2591-2600, https://doi.org/10.1039/C7CY00529F.
58. Fan, X.; Tian, J.; Cheng, R. MoS_2 quantum dot decorated g-C_3N_4 composite photocatalyst with enhanced hydrogen evolution performance. *RSC Advances* **2016**, *6*, 52611-52619, https://doi.org/10.1039/C6RA07060D.
59. Chen, B.; Zhou, L.; Liu, Y. Inverse opal TiO_2/g-C_3N_4 composite with heterojunctions construction for enhanced visible light driven photocatalytic activity. *Dalton Trans* **2019**, *48*, 3486-3495, https://doi.org/10.1039/C8DT04496A.
60. Huang, L.; Li, Y.; Xu, Y. Visible light induced WO_3/g-C_3N_4 composites with enhanced photocatalytic activity. *Dalton Transactions* **2013**, *42*, 8606-8616, https://doi.org/10.1039/C3DT00115F.
61. Zhang, P.; Lou, Z.; Shi, X. In situ nitrogen doped hollow TiO_2/g-C_3N_4 composite photocatalysts with efficient charge separation boosting water reduction under visible light. *Journal of Materials Chemistry A* **2017**, *5*, 9671-9681, https://doi.org/10.1039/C7TA01888F.
62. Ni, Z.; Liu, X.; Su, N. Ultrasound assisted two step water bath synthesis of g-C_3N_4/BiOBr composites visible light driven photocatalysis sterilization and reaction mechanism. *New Journal of Chemistry* **2019**, *43*, 8711, http://dx.doi.org/10.1039/C9NJ01398A.
63. Gan, Z.; Zhou, W.; Ding, Z. A metal free 3C-SiC/g-C_3N_4 composite with enhanced visible light photocatalytic activity. *RSC Advances* **2017**, *7,* 40028-40033, https://doi.org/10.1039/C7RA06497G.
64. Han, C.; Liu, J. Insitu synthesis and enhanced visible light photocatalytic activities of novel PANI-g-C_3N_4 composite photocatalysts. *Journal of Mataerials Chemistry* **2012**, *22,* 11843-11850, https://doi.org/10.1039/C2JM16241E.

6. ACKNOWLEDGEMENTS

Authors are thankful to the management SOA (deemed to be University) for constant encouragement.